FABAD J. Pharm. Sci., 47, 2, 201-212, 2022
Doi: 10.55262/fabadeczacilik.1134568
RESEARCH ARTICLE

Fabrication and Evaluation of Cationic Charged Magnetic Nanoparticles for Enhanced Gene Delivery

Hasan AKBABA[*°], Gülşah EREL-AKBABA[**], Ayşe Gülten KANTARCI[***]

Fabrication and Evaluation of Cationic Charged Magnetic Nanoparticles for Enhanced Gene Delivery

SUMMARY

Magnetofection; represents nucleic acid delivery by using magnetic nanoparticles (MNPs) under the influence of a magnetic field; gives promising results for gene delivery. However, pharmaceutical and biomedical studies in this area are very limited. To meet this need, we aimed to develop an effective magnetic gene delivery system in this study. The in-situ surface coating method was handled to develop cationic charged MNPs. Three different MNP formulations were obtained and investigated in terms of characterization, DNA binding, protection, and transfection ability. According to the results, the obtained MNPs have particles under 150 nm with a low PDI (<0.3), and positive zeta potential with a spherical shape. The DNA binding and protecting ability from nucleases were shown by agarose gel studies. No significant cytotoxicity was observed on COS-7 cells in the concentration range of 4-20 µL/well. Moreover, transfection studies revealed that the optimal system (GMS-MNP-1) showed significantly higher transfection efficacy comparing the naked plasmid or non-magnetic version of nanoparticle under a magnetic field (p>0.05). Promising results have been obtained with the use of obtained GMS-MNPs in terms of magnetic gene delivery. This work can be extended to in vivo by using disease-specific therapeutic genetic materials.

Key Words: *Gene delivery, magnetofection, cytotoxicity, transfection*

Gelişmiş Gen Teslimatı için Katyonik Yüklü Manyetik Nanopartiküllerin İmalatı ve Değerlendirilmesi

ÖZ

Manyetofeksiyon; manyetik alanın etkisi altında manyetik nanopartiküller (MNP'ler) kullanılarak nükleik asit aktarımı olarak tanımlanan, gen terapisi için umut verici sonuçlar veren bir tekniktir. Ancak bu alandaki farmasötik ve biyomedikal çalışmalar oldukça sınırlıdır. Bu ihtiyacı karşılanması için çalışmamıda etkili bir manyetik gen aktarım sistemi geliştirmeyi amaçladık. Katyonik yüklü MNP'lerin geliştirilmesi için yerinde yüzey kaplama yöntemi kullanıldı. Üç farklı MNP formülasyonu elde edildi ve karakterizasyon, DNA ile kompleks oluşturma, koruma ve transfeksiyon etkinliği açısından araştırıldı. Sonuçlara göre, elde edilen MNP'lerin 150 nm'nin altında, düşük PDI değerinde (<0.3) ve pozitif zeta potansiyelde küresel partiküller oldukları gösterildi. DNA ile kompleks oluşturma ve nükleazlardan DNA'yı koruma yeteneği, agaroz jel çalışmaları ile gösterildi. 4-20 µL/kuyucuk konsantrasyon aralığında COS-7 hücrelerinde önemli bir sitotoksisite gözlenmedi. Ayrıca, transfeksiyon çalışmaları, optimal olarak belirlenen sistemin (GMS-MNP-1), manyetik alan altında çıplak plazmit veya nanopartikülün manyetik olmayan versiyonuna kıyasla önemli ölçüde daha yüksek transfeksiyon etkinliği gösterdiğini ortaya koydu (p>0.05). Elde edilen GMS-MNP'lerin manyetik gen aktarımı açısından kullanılmasıyla umut verici sonuçlar elde edilmiştir. Bu çalışma, hastalığa özgü terapötik genetik materyaller kullanılarak in vivo olarak genişletilebilir.

Anahtar Kelimeler: *Gen aktarımı, manyetofeksiyon, sitotoksisite, transfeksiyon*

Received: 17.01.2022
Revised: 18.04.2022
Accepted: 05.05.2022

[*] ORCID: 0000-0001-9273-6346,Ege University, Faculty of Pharmacy, Department of Pharmaceutical Biotechnology, İzmir, Turkey
[**] ORCID: 0000-0003-3287-5277, Izmir Katip Celebi University, Faculty of Pharmacy, Department of Pharmaceutical Biotechnology, İzmir, Turkey
[***] ORCID: 0000-0001-8813-5353, Ege University, Faculty of Pharmacy, Department of Pharmaceutical Biotechnology, İzmir, Turkey

[°] Corresponding Author; Hasan AKBABA
Ege University, Faculty of Pharmacy, Department of Pharmaceutical Biotechnology, İzmir, Turkey
Tel. +90 5354026155, e.mail: hasan.akbaba@ege.edu.tr

INTRODUCTION

Nanotechnology covers the applications of new substances, materials, and methods developed by using nanometer-sized materials in medicine, engineering, pharmacy, physics, and many other sciences. It finds wider application areas, especially in molecular science and biomedicine (Kami et al., 2011). Since nanoparticles are small enough to easily enter almost all body areas, including the circulatory system and cells, they have become the basis of basic biomedical research, diagnostic science, and therapeutic applications of nanotechnology (Selmani et al., 2022).

In gene therapy, the therapeutic genes to be transferred have to deal with intracellular and extracellular barriers. Intracellular barriers originate from the cell, including the cell membrane, endosome, and nuclear membrane. On the other hand, extracellular barriers include serum proteins, nuclease enzymes, and the body's defense system. All these obstacles significantly reduce the efficiency of gene transfer (Sharma et al., 2021). Vector systems have been developed to overcome these barriers and ensure efficient gene transport (Foldvari et al., 2016).

Due to the safety and efficacy problems encountered in various gene transfer techniques, magnetic nanoparticle (MNP) applications have been oriented towards gene transfer over time. The beginnings of MNP-based transfection methods date back to the research of magnetically targetable drug delivery systems by Widdler et al in the late 1970s (McBain et al., 2008). This method is based on the principle that the therapeutic agent is attached to micro or nano-sized particle with magnetic properties or is entrapped in these particles. By modifying the surface properties of the MNP, it is possible to bind the drug or DNA on it and direct it to the target tissues and cells. Targeting a cytotoxic treatment agent directly to the chemotherapy site or directing the therapeutic DNA to the genetic disordered area are some examples of MNPs applications (Bi et al., 2020).

In many studies, it has been proven that gene transfer under a magnetic field by using MNPs; also called magnetofection; increases transfection efficiency (Kami et al., 2011). This technique is based on the binding of genetic material to MNPs. For MNP-based *in vitro* transfection, the particle-DNA complex is applied to the cell culture and a magnet or electromagnet is placed on the underside of this cell culture, which can generate a magnet-like electromagnetic field. Thus, the sedimentation and transfection rate of the DNA-particle complex increases (Dowaidar et al., 2017).

The total surface charge and the size of the MNP nucleic acid complex play essential roles in the cellular uptake of cells (Jin & Kim, 2014). For this purpose, cationic lipid coating strategies are applied to MNPs to form complexes with oppositely charged nucleic acids via electrostatic interaction, where nucleic acids are considered negatively charged molecules due to their phosphate groups (He et al., 2007; Song et al., 2010).

Many routes have been developed to synthesize MNPs, which are popular options in medical applications. In this study, the *in-situ* surface coating method was handled to develop cationic charged MNPs for gene delivery. Three different MNP formulation was obtained and investigated in terms of characterization, DNA binding, protection, and transfection ability.

MATERIAL AND METHODS

Green fluorescent protein-encoding plasmid (pEGFP-C1) was purchased from Invitrogen, USA. The pEGFP-C1 was amplified in the *DH5α* strain of *E. coli* and extracted by Gene Jet Endo-free plasmid maxiprep kit (Thermo Scientific, USA).

Glyceryl monostearate (GMS) and Kolliphor HS15 were obtained from BASF, Germany. Ethanol, Tween 80, $FeCl_{2,}$ and $FeCl_3$ were provided by Merck- Co. (Hohenbrunn, Germany). Cremephor RH40, Span 80, and dimethyl dioctadecyl ammonium bro-

mide (DDAB) were purchased from Sigma-Aldrich Co. (St. Louis, MO, USA). XTT cell proliferation assay kit was obtained from Thermo Fisher Scientific (MA, USA). African green monkey kidney fibroblast-like cell line (COS-7) cell line was purchased from ATCC. All other chemicals were used as an analytical grade.

MNP Synthesis

Three different MNP formulations were developed by using the combination of microemulsion and multiple emulsion techniques. MNPs were synthesized in the core of multiple emulsions. GMS and DDAB were used as the main solid lipid and cationic lipid, respectively for all three formulations as the 1:1 weight ratio.

As the first step for magnetic nanoparticle preparation, the triangle phase diagram of water in oil (w_1/o) microemulsion was obtained at 10°C higher than the solid lipid melting point (Akbaba et al., 2017). Different surfactant and co-surfactant components used for magnetic nanoparticle synthesis was given in Table 1. Fe^{+2} and Fe^{+3} solutions were used as internal water phase (w_1/o) in all formulations. Transparent regions belonging to w_1/o microemulsion area were drawn in phase diagrams. DDAB was incorporated into the oil phase of the microemulsion for gaining cationic property to the MNPs. The obtained microemulsion was used as an interior emulsion of multiple emulsions (w_1/o/w_2). Then, by using an outer surfactant and ultrapure water, multiple emulsion was obtained. The pH of the system was increased by using 1 N NaOH and by leaking [OH^-] ions to the interior water phase of the multiple emulsion, magnetic iron oxide particles were synthesized in the core of cationic lipids (Schmidts et al., 2010).

Table 1. Compositions of developed magnetic nanoparticle formulations. (S_1:surfactant$_1$; Co-S:co-surfactant; S_2:surfactant$_2$; w/w: weight/weight)

Formulation code	GMS	DDAB	S_1	Co-S	S_1:Co-S (w/w)	S_2
GMS-MNP-1	+	+	S80:T80	EtOH	1:3	T80
GMS-MNP-2	+	+	S80:HS15	EtOH	1:3	HS15
GMS-MNP-3	+	+	S80:RH40	EtOH	1:3	RH40

As the last step for MNP development, 1 mL of hot multiple emulsion with magnetic core was dispersed into the ice-cold distilled water (0-2°C). MNPs were formed when multiple emulsion droplets met with cold water (Akbaba et al., 2018; Cavalli et al., 2000). A neodymium magnet was used for the separation of GMS-MNPs. GMS-MNPs were washed with UPH_2O two times and redispersed in UPH_2O. The final concentration was 25 mg/mL, with respect to solid lipids for all GMS-MNP formulations.

Characterization

Magnetic properties of GMS-MNPs were confirmed by using Lakeshore Vibrating Sample Magnetometer (VSM). Moreover, the particle size and zeta potential of nanoparticles were evaluated with the dynamic light scattering (DLS) method. For this purpose, Zetasizer Nano ZS (Malvern Instruments, Worcestershire, U.K.) was used. Experiments were carried out at least in triplicate. The morphology of GMS-MNPs was further evaluated by Transmission Electron Microscope (TEM, FEI Tecnai G2 Spirit BioTwin CTEM, Oregon, USA) for visualizing the samples.

Confirmation of complex formation ability

GMS-MNPs were complexed with pEGFP-C1 through electrostatic interactions between cationic lipids in the nanoparticles and anionic phosphate groups in the DNA. For this purpose, 3 µL GMS-MNPs (containing 25 mg/mL with respect to solid lipids) was added onto the 1 µL pEGFP-C1 solution (100 ng/µL) and incubated for 30 minutes on a benchtop shaker at 25 °C. Complex formation was checked by agarose gel electrophoreses. Agarose gel was prepared in 1 x tris-acetate-EDTA (TAE) buffer

as the final agarose concentration 1% (w/v) and the gel was run for 60 minutes at 100 V. To visualize; the gel was stained with ethidium bromide (0.5 µg/ml in UpH_2O) and photographed with UV transilluminator (Syngene, UV Transilluminator, USA).

Evaluation of protection ability

Another important parameter to achieving gene delivery is protecting the transported nucleic acids against nuclease enzymes. To evaluate this ability, GMS-MNPs and pEGFP-C1 were first complexed as explained above. Following the complex formation, 0.4 IU DNase I (New England Biolabs, USA) was added per each 1 µg DNA and incubated for 30 minutes in a 37 °C incubator to mimic body temperature (Capan et al., 1999; del Pozo-Rodríguez et al., 2009). At the end of the incubation period, SDS (1%) was added onto the complex to release the DNA (Erel-Akbaba & Akbaba, 2021). The released pEGFP-C1 was visualized by agarose gel electrophoreses and the degradation percentage was calculated via Image J software. As a control, GMS-MNPs were also complexed with the same amount of pEGFP-C1 and released by using SDS without incubating DNase I for all formulations.

Cytotoxicity profiles

Cytotoxicity profiles of obtained GMS-MNPs and GMS-MNP:pEGFP-C1 complexes were evaluated on COS-7 cell line. For this purpose, the cells were cultured in complete media containing Dulbecco's Modified Eagle's Medium (DMEM, low glucose) with 10% fetal bovine serum (FBS) and penicillin– streptomycin (100 UI/ml penicillin, 100 µg/ml streptomycin).

COS-7 cells were seeded into 96 well plates at the concentration $1x10^5$ cells/well and incubated overnight in a 5% CO_2 atmosphere at 37 °C. The following day, the medium was replaced with fresh DMEM that contains 4, 8, 12, 16, and 20 µL/well formulations and further incubated for 24 h. The highest three equivalent doses for each GMS-MNP were also evaluated for the complex forms in terms of cytotoxicity.

At the end of the incubation period, XTT cell proliferation assay kit protocol (Biological Industries, Israel) was performed by using Thermo Varioscan multiplate reader (Thermo, USA). The viability of cells was calculated by normalizing the fluorescence of untreated cells. Experiments were performed in quadruplicate.

Evaluation of transfection ability

The transfection ability of obtained formulations was evaluated on COS-7 cell line by using fluorescence microscopy and flow cytometry. For this purpose, cells were seeded in 6-well culture plates at a density of $5x10^4$ cells/ml and incubated overnight. To perform transfection, the 2.5 µg pEGFP-C1 plasmid was complexed with GMS-MNPs at the 3:1 volume ratio and applied to the cells. As a control group, the transfection ability of the naked pEGFP-C1 plasmid was also evaluated.

The cells were incubated for 4 h with formulations. At the end of the 4 h, the medium was removed and a fresh growth medium was added. The cells were allowed to grow and protein synthesis for a further 48 h. The transfection was first visualized by fluorescence microscopy (IX71, Olympus, Tokyo, Japan). Subsequently, flow cytometric analysis was also performed to detect the green fluorescence protein signal which occurs in the transfected cells. For flow cytometry, the cells were trypsinized and harvested, then washed twice with phosphate-buffered saline (PBS) and suspended in 100 µl FACs buffer (2% calf serum in PBS) Flow cytometry was performed by BD Accuri™ C5 (AZ, USA). Data corresponding to 10,000 events were collected for every group and analyzed with BD CFlow software (AZ, USA).

Statistical analysis

Data were expressed as mean ± standard error of the mean (SEM). A non-paired t-test and one-way variance analysis (ANOVA) followed by multiple comparison tests were used to evaluate the statistical analysis between the groups. A p-value < 0.05 was considered as significant.

RESULTS AND DISCUSSION

The multiple emulsion technique was handled in this study to develop GMS-MNPs. For this purpose, (w_1/o) microemulsion phase diagrams were determined as given in Figure 1. According to the triangular diagrams, the formulation ratios contained the largest volume of inner water phase was selected and used for the formation of magnetic nanoparticles. To ensure the magnetic properties of the developed formulation, VSM studies were performed as well (Figure 2).

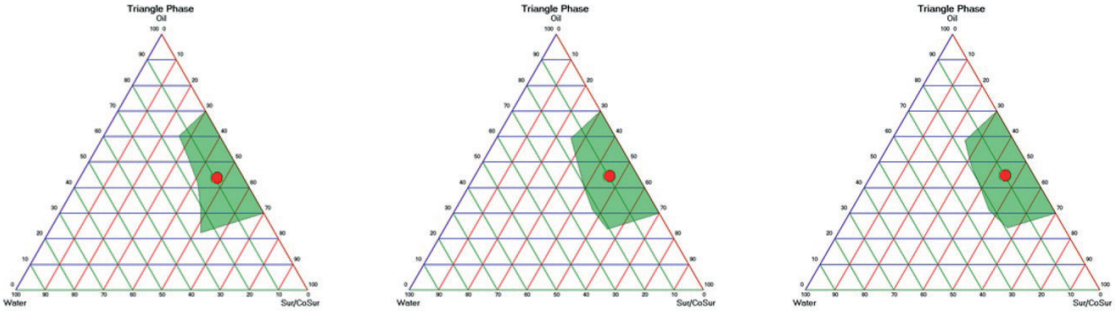

GMS-MNP-1 **GMS-MNP-2** **GMS-MNP-3**

Figure 1. Triangular phase diagram of w_1/o microemulsion formed with GMS as oil phase, Fe^{+2} and Fe^{+3} solutions as water phase, and various S/Co-S mixtures. The Green area shows a transparent w_1/o microemulsion region.

The regions of transparent microemulsion formation have a similar area for both formulations. The main parameter of this formation is that the HLB values are the same for each surfactant mixture which is equivalent to 5.58. Since the clear w_1/o microemulsion will then be used as the inner phase of the o/w_2 emulsion, it is important that it should be stable.

Following stable w_1/o microemulsion formation, the MNPs have formed as explained in the materials and methods section. The obtained MNPs were characterized in terms of size, polydispersity index (PDI), and zeta potential (Table 2). The ideal nanoparticle size may be different depending on the targeting tissue, for example, smaller size nanoparticle production is required to overcome the blood–brain barrier, as well as bigger nanoparticles, are needed for lung accumulation. According to the characterization results, the particle sizes of obtained GMS-MNPs were measured under 150 nm and PDI's were under 0.3 which is important for showing nanoparticles uniformity in terms of the size distribution (Elsana et al., 2019). Zeta potential values of GMS-MNPs were determined positive (above +20 mV) for all three formulations as expected. This charge is further used to complex pEGFP-C1 plasmid to the outer surface of nanoparticles through electrostatic interactions (Ozder & Akbaba, 2021). Moreover, TEM images supported that all GMS-MNPs are nano-sized and in globular structure (Figure 2).

Table 2. Characterization results for prepared MNP formulations as mean ± standard deviation (SD) (n=3).

Formulation	Particle size (nm ± SD)	PDI (± SD)	Zeta Potential (mV ± SD)
GMS-MNP-1	139.9 ± 2.9	0.160 ±0.023	41.1 ± 1.6
GMS-MNP-2	185.5 ± 1.5	0.158 ±0.011	20.7 ± 0.8
GMS-MNP-3	214.4 ± 2.7	0.255 ±0.076	20.2 ± 2.7
GMS-MNP-1:pEGFP-C1 (3:1, v/v)	427.7 ± 21.5	0.327 ±0.066	30.6 ± 1.07
GMS-MNP-2:pEGFP-C1 (3:1, v/v)	550,0 ± 36.8	0.659 ±0.062	37.8 ± 3.10
GMS-MNP-3:pEGFP-C1 (3:1, v/v)	397.7 ± 8.1	0.511 ±0.027	29.4 ± 3.05

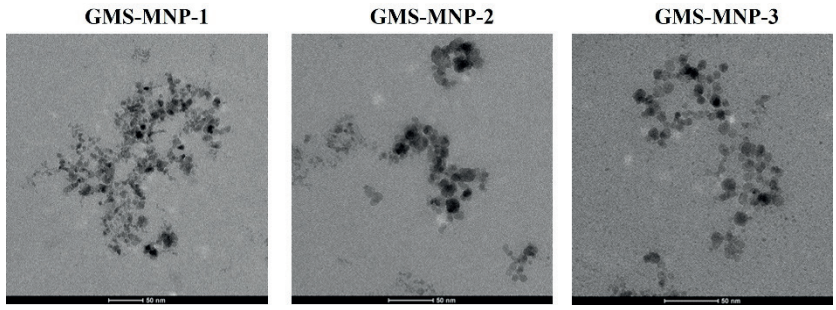

Figure 2. Morphological examination of GMS-MNPs. Scale bars represent 50 nm.

The magnetic properties of the nanoparticles obtained after the formation of the multiple emulsion and subsequent pH increase and washing were analyzed by VSM. An ideal magnetic nanoparticle should be paramagnetic (Gupta & Gupta, 2005; Tombácz et al., 2015). The magnetic properties such as saturation magnetization (Ms), remanent magnetization (Mr), and coercivity (Hc) were evaluated from the magnetization hysteresis of GMS-MNPs (Gupta & Gupta, 2005; Tombácz et al., 2015; Zhi et al., 2006).

As seen in Figure 3, all three formulations are in paramagnetic behavior and Mr and Hc values are approximately zero. According to the literature, saturation magnetization of magnetite is higher than in the coated samples we prepared. However, GMS-MNPs have reasonably sufficient Ms values for magnetic targeting of nucleic acids (Sun et al., 2008). Ms values were measured as 15, 10, and 8 emu g^{-1} for lipid-coated GMS-MNP-1, GMS-MNP-2, and GMS-MNP-3, respectively.

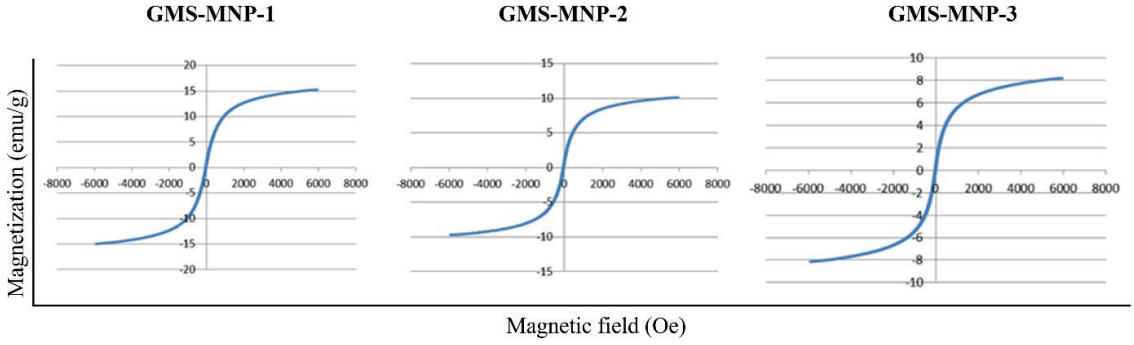

Figure 3. Magnetization hysteresis loops of GMS-MNP-1, GMS-MNP-2 and, GMS-MNP-3.

Agarose gel electrophoresis studies were carried on to confirm the complex formation via pDNA and determine the protection ability of the formulation against the degradation of nucleases (Figure 4). All three GMS-MNPs were interacted electrostatically with the pEGFP-C1 plasmid and blocked the DNA mobility on agarose gel electrophoresis at a ratio of 3:1 (v/v). The obtained GMS-MNP-1:pEGFP-C1 (3:1, v/v) were further characterized. As seen in Table 2, the particle sizes and PDI values of the complexed formulations were increased. This was an expected result, as DNA binds to the outer surface of the nanoparticles. On the other hand, the zeta potential remained positive. This may be adventageus for transfection as the positively charged nanoparticles could easily interact with the negatively charged cell membrane (Gan et al., 2005).

Stereological protection of the particles against the degradation of the DNase enzyme is required for

an effective transfection (Capan et al., 1999; del Pozo-Rodríguez et al., 2010). First of all, the efficacy of SDS in releasing pDNA from the complex was evaluated. As seen in Figure 4b, the pEGFP-C1 was successfully released from the complex with the help of SDS, for all formulations.

Figure 4c shows the results of the gel electrophoresis study involving the samples treated with DNase I. The bands were observed and the integrity of the GMS-MNPs were compared with a control of untreated pEGFP-C1 in lane 1 and naked pEGFP-C1 was threatened with the same amount of *DNase I* as control of enzyme activity in lane 2. The band densities were quantified with ImageJ Software and degradation percentages were calculated according to the control groups. Naked pEGFP-C1 was totally degraded after *DNase I* treatment. However, GMS-MNPs were protected pEGFP-C1 in various levels. The non-degraded pEGFP-C1 percentage after complex formation with GMS-MNP-1 was calculated as 71.7 %, for GMS-MNP-2 it was calculated as 77.9 %, and for GMS-MNP-3 it was calculated as 23.5 %.

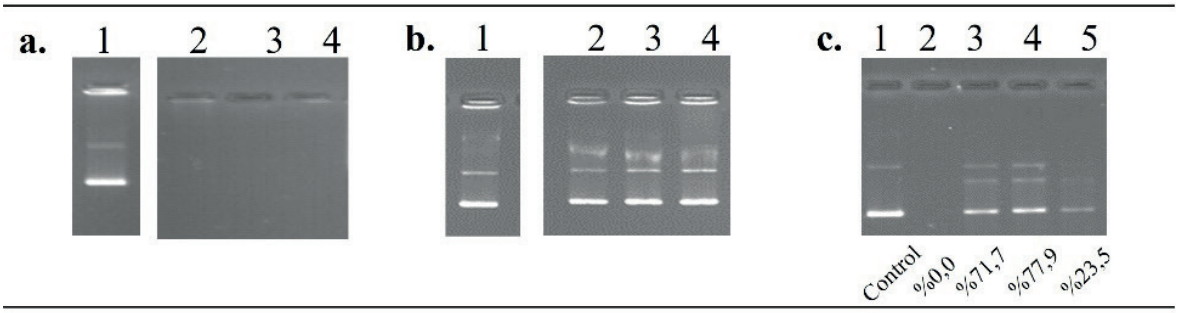

Figure 4. Gel retardation and DNase I protection studies agarose gel images. **a.** Confirmation of complex formation ability of GMS-MNP-1,2, and 3 (Lanes from left 1: naked pEGFP-C1 (100 ng/well); 2-4: GMS-MNP-1, 2, and 3 :pEGFP-C1 (3:1, v/v) complexes). **b.** Efficacy of SDS to release pEGFP-C1 from GMS-MNP: pEGFP-C1 complexes (Lanes from left 1: naked pEGFP-C1 (100 ng/well); 2-4: released pEGFP-C1 from GMS-MNP-1, 2, and 3 :pEGFP-C1 (3:1, v/v) complexes). **c.** DNase I degradation of GMS-MNPs. (Lanes from left 1: naked pEGFP-C1 (100 ng/well); 2: naked pEGFP-C1 + *DNase I* enzyme; 3–5: GMS-MNP-1, 2, and 3 complexes + *DNase I* enzyme).

Non-cytotoxic behavior of the developed system is another critical factor for formulation development studies. (Abas et al., 2021; Erel-Akbaba et al., 2020). According to the results of the cytotoxicity assay, no significant cytotoxicity was observed on COS-7 cells in the concentration range of 4-20 µL/well for GMS-MNP-1 and GMS-MNP-3 formulations (Figure 5). A dose-dependent decrease in cell viability was observed for GMS-MNP-2 formulation. The highest three equivalent doses for each GMS-MNP were also evaluated for each complex form in terms of cytotoxicity and the viability of the cells dramatically increased for the GMS-MNP-2 formulation. Considering the stereological protection and cytotoxicity studies, the GMS-MNP-1 formulation was determined to be superior to the GMS-MNP-2 and GMS-MNP-3 formulations in both conditions. However, the efficiency of transfection is one of the most important parameters to evaluate.

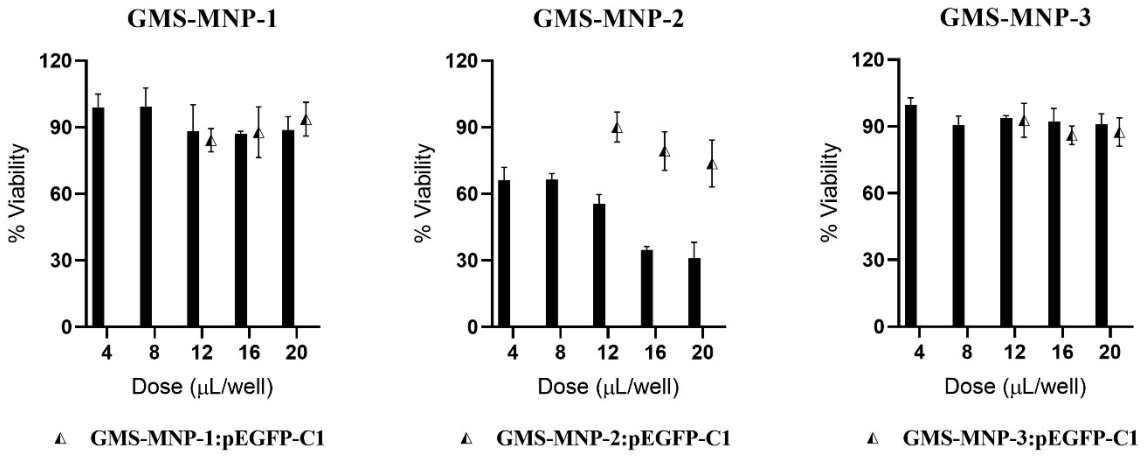

Figure 5. Cytotoxicity evaluation of GMS-MNPs and GMS-MNP:pEGFP-C1 (3:1, v/v) complexes

The ability and efficiency of transfection were evaluated both qualitatively and quantitatively. EGFP, which is the expression product of the pEGFP-C1 plasmid, has a single excitation peak centered at about 488 nm, with an emission peak wavelength of 509 nm excitation peak (del Pozo-Rodríguez et al., 2010). EGFP expressed by cells was visualized under an appropriate filter using fluorescence microscopy (IX71, Olympus, Tokyo, Japan) (Figure 6). Commercially available magnetofection agent PolyMag was used as a positive control. In order to observe the effect of magnetic field on transfection, the formulation containing UPH_2O instead of Fe solution in the inner aqueous phase was also added to the experimental protocol as a control together with naked pEGFP-C1 plasmid. According to fluorescence microscope images, although it is relatively higher in the GMS-MNP-1 formulation, similar levels of EGFP expression were observed in the GMS-MNP-2 and GMS-MNP-3 formulations, as well as PolyMag. The non-magnetic version of GMS-MNP-1 (called as GMS-NPS-1) formulation showed a significantly low level of transfection and no fluorescence signal was observed with the naked pEGFP-C1 ($p<0.05$). It can be deduced from the fluorescence microscopy results that the application of a magnetic field increases the transfection ability.

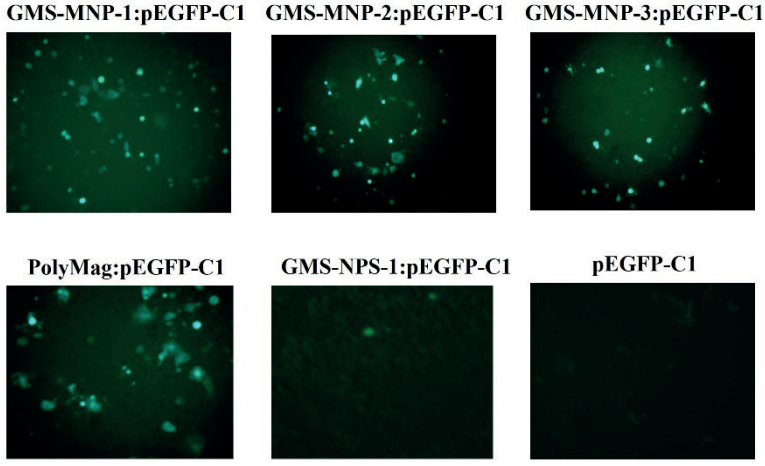

Figure 6. Qualitative magnetofection ability of GMS-MNPs, GMS-NP, and naked pEGFP-C1 plasmid. Images of EGFP-positive cells under a fluorescence microscope.

In order to demonstrate the transfection efficiency quantitatively, flow cytometry was performed under the blue laser (Figure 7). Obtained results are in parallel with the fluorescence microscopy images. Transfection efficiency was measured as 30.1% for GMS-MNP-1, 23.0% for GMS-MNP-2, and 26% for GMS-MNP-3. The transfection efficiency of GMS-MNP-1 is similar to the commercial product PolyMag (30.2%) used as a positive control. The transfection efficiency was found to be significantly lower for naked pEGFP-C1 (4.9 %).

Briefly, MNP-GMS-1 formulation is suggested as an optimal formulation considering its characteristics, stereological protection, toxicity, and magnetofection efficiency comparing MNP-GMS-2 and 3.

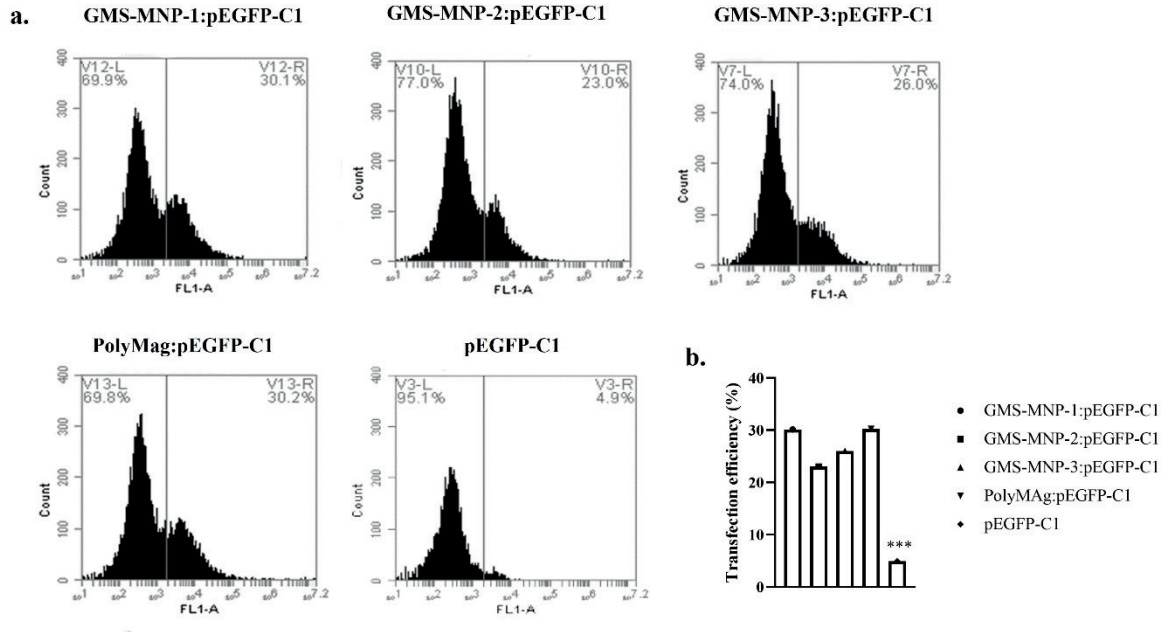

Figure 7. Representative flow cytometry histograms of transfection study groups (a). Quantitative analysis of EGFP expression percentage in COS-7 cells by flow cytometry analysis (b).

Targeted therapy with magnetic nanoparticles is an intriguing subject. As the novel genetic mechanisms were identified, the need for targeting these structures in the tissues or cells is increasing proportionally (Aslam et al., 2022). Magnetofection, one of the active drug targeting methods, attracts the attention of researchers as an important method to overcome this challenge.

In recent years, various studies on MNP-mediated gene targeting, especially cancer cell targeting, have been published. In one of these, polyethyleneimine-coated magnetic nanoparticles were designed to silence the overexpressed MUC1 gene in breast cancer. The developed MNPs have a particle size of 200 nm to 400 nm, similar to developed GMS-MNPs in our study (Amani et al., 2021). Another study focused on magnetic nanoparticles to target CRISPR/dCas9 ribonucleoproteins. MNP were coated with chitosan to deliver the CRISPR/dCas9 ribonucleoproteins, however, particle size of the developed system reached micron sizes (Lee et al., 2021). In another study, researchers investigated the performance of microcarriers as drug delivery systems that were applied to each branch of the lung under the influence of a magnetic field in terms of delivery of the drugs after the respiratory syndromes of Covid-19 (Ebrahimi et al., 2021). Although MNP synthesis using emulsion technology is a known method, it should be noted as a

novelty that no study has been encountered that provides lipid coating with in situ MNP synthesis.

CONCLUSION

To sum up, GMS-MNP formulations with 3 different surfactant compositions were developed and evaluated in parallel. Obtained GMS-MNPs are paramagnetic and have the ability to target genetic material under a magnetic field. However, GMS-MNP-1 formulation is suggested as an optimal formulation considering its characteristics, stereological protection, toxicity, and magnetofection efficiency in comparison to GMS-MNP-2 and GMS-MNP-3. Expanding studies on therapeutic genetic material delivery under the magnetic field and evaluating its *in vivo* potential are the future goals of this study.

ACKNOWLEDGEMENTS

This study has been financially supported by the Scientific and Technological Research Council of Turkey (TÜBİTAK) under grant code TÜBİTAK-SBAG-112S2942.

CONFLICT OF INTEREST

None of the authors of this paper has a financial or personal relationship with other people or organizations that could inappropriately influence or bias the content of the paper.

No Competing interests are at stake and there is No Conflict of Interest" with other people or organizations that could inappropriately influence or bias the content of the paper.

AUTHOR CONTRIBUTION STATEMENT

All authors have given approval for the final version of the manuscript. H.A. and G.E-A. carried out the experiments. H.A. and G.E-A. wrote the manuscript with support from A.G.K. H.A. conceived the original idea. A.G.K. supervised the project. All authors contributed to this work presented in this manuscript.

REFERENCES

Akbaba, H., Erel Akbaba, G., & Kantarcı, A. G. (2018). Development and evaluation of antisense shRNA-encoding plasmid loaded solid lipid nanoparticles against 5-α reductase activity. *Journal of Drug Delivery Science and Technology*, *44*(August 2017), 270–277. https://doi.org/10.1016/j.jddst.2018.01.001

Akbaba, H., Karagöz, U., Selamet, Y., & Kantarcı, A. G. (2017). Synthesis and characterization of cationic lipid coated magnetic nanoparticles using multiple emulsions as microreactors. *Journal of Magnetism and Magnetic Materials*, *426*(November 2016), 518–524. https://doi.org/10.1016/j.jmmm.2016.11.126

Amani, A., Alizadeh, M. R., Yaghoubi, H., & Ebrahimi, H. A. (2021). Design and fabrication of novel multi-targeted magnetic nanoparticles for gene delivery to breast cancer cells. *Journal of Drug Delivery Science and Technology*, *61*, 1773–2247. https://doi.org/10.1016/J.JDDST.2020.102151

Aslam, H., Shukrullah, S., Naz, M. Y., Fatima, H., Hussain, H., Ullah, S., & Assiri, M. A. (2022). Current and future perspectives of multifunctional magnetic nanoparticles based controlled drug delivery systems. *Journal of Drug Delivery Science and Technology*, *67*, 102946. https://doi.org/10.1016/J.JDDST.2021.102946

Bi, Q., Song, X., Hu, A., Luo, T., Jin, R., Ai, H., & Nie, Y. (2020). Magnetofection: Magic magnetic nanoparticles for efficient gene delivery. *Chinese Chemical Letters*, *31*(12), 3041–3046. https://doi.org/10.1016/j.cclet.2020.07.030

Capan, Y., Woo, B. H., Gebrekidan, S., Ahmed, S., & DeLuca, P. P. (1999). Stability of poly(L-lysine)-complexed plasmid DNA during mechanical stress and DNase I treatment. *Pharmaceutical Development and Technology*, *4*(4), 491–498. https://doi.org/10.1081/PDT-100101386

Cavalli, R., Caputo, O., & Gasco, M. R. (2000). Preparation and characterization of solid lipid nanospheres containing paclitaxel. *European Journal of Pharmaceutical Sciences*, *10*(4), 305–309. https://doi.org/10.1016/S0928-0987(00)00081-6

del Pozo-Rodríguez, A., Delgado, D., Solinís, M. Á., Pedraz, J. L., Echevarría, E., Rodríguez, J. M., & Gascón, A. R. (2010). Solid lipid nanoparticles as potential tools for gene therapy: In vivo protein expression after intravenous administration. *International Journal of Pharmaceutics*, *385*(1–2), 157–162. https://doi.org/10.1016/J.IJPHARM.2009.10.020

del Pozo-Rodríguez, A., Pujals, S., Delgado, D., Solinís, M. A., Gascón, A. R., Giralt, E., & Pedraz, J. L. (2009). A proline-rich peptide improves cell transfection of solid lipid nanoparticle-based non-viral vectors. *Journal of Controlled Release*, *133*(1), 52–59. https://doi.org/10.1016/j.jconrel.2008.09.004

Dowaidar, M., Abdelhamid, H. N., Hällbrink, M., Freimann, K., Kurrikoff, K., Zou, X., & Langel, Ü. (2017). Magnetic Nanoparticle Assisted Self-assembly of Cell Penetrating Peptides-Oligonucleotides Complexes for Gene Delivery. *Scientific Reports*, *7*(1). https://doi.org/10.1038/s41598-017-09803-z

Ebrahimi, S., Shamloo, A., Alishiri, M., Mofrad, Y. M., & Akherati, F. (2021). Targeted pulmonary drug delivery in coronavirus disease (COVID-19) therapy: A patient-specific in silico study based on magnetic nanoparticles-coated microcarriers adhesion. *International Journal of Pharmaceutics*, *609*, 121133. https://doi.org/10.1016/J.IJPHARM.2021.121133

Elsana, H., Olusanya, T. O. B., Carr-wilkinson, J., Darby, S., Faheem, A., & Elkordy, A. A. (2019). Evaluation of novel cationic gene based liposomes with cyclodextrin prepared by thin film hydration and microfluidic systems. *Scientific Reports*, *9*(1), 1–17. https://doi.org/10.1038/s41598-019-51065-4

Erel-Akbaba, G., & Akbaba, H. (2021). Investigation of the potential therapeutic effect of cationic lipoplex mediated fibroblast growth factor-2 encoding plasmid DNA delivery on wound healing. *DARU Journal of Pharmaceutical Sciences*, *0123456789*. https://doi.org/10.1007/s40199-021-00410-y

Erel-Akbaba, G., Öztürk, İ., & Ay-Şenyiğit, Z. (2020). Improvement of the Antimicrobial Activity of Moxifloxacin Using W/O Microemulsion System for Skin Infections. *FABAD Journal of Pharmaceutical Sciences*, 45 (3), 219-227.

Foldvari, M., Chen, D. W., Nafissi, N., Calderon, D., Narsineni, L., & Rafiee, A. (2016). Non-viral gene therapy: Gains and challenges of non-invasive administration methods. *Journal of Controlled Release*, *240*, 165–190. https://doi.org/10.1016/J.JCONREL.2015.12.012

Gan, Q., Wang, T., Cochrane, C., & McCarron, P. (2005). Modulation of surface charge, particle size and morphological properties of chitosan-TPP nanoparticles intended for gene delivery. *Colloids and Surfaces. B, Biointerfaces*, *44*(2–3), 65–73. https://doi.org/10.1016/j.colsurfb.2005.06.001

Gupta, A. K., & Gupta, M. (2005). Synthesis and surface engineering of iron oxide nanoparticles for biomedical applications. *Biomaterials*, *26*(18), 3995–4021. https://doi.org/10.1016/j.biomaterials.2004.10.012

He, X., Huo, H., Wang, K., Tan, W., Gong, P., & Ge, J. (2007). Plasmid DNA isolation using amino-silica coated magnetic nanoparticles (ASMNPs). *Talanta*, *73*(4), 764–769. https://doi.org/10.1016/J.TALANTA.2007.04.056

Jin, S. E., & Kim, C. K. (2014). Charge-mediated topical delivery of plasmid DNA with cationic lipid nanoparticles to the skin. *Colloids and Surfaces B: Biointerfaces*, *116*, 582–590. https://doi.org/10.1016/J.COLSURFB.2014.01.053

Kami, D., Takeda, S., Itakura, Y., Gojo, S., Watanabe, M., & Toyoda, M. (2011). Application of magnetic nanoparticles to gene delivery. *International Journal of Molecular Sciences*, *12*(6), 3705–3722. https://doi.org/10.3390/ijms12063705

Lee, M. H., Lin, C. C., Thomas, J. L., Li, J. A., & Lin, H. Y. (2021). Cellular reprogramming with multigene activation by the delivery of CRISPR/dCas9 ribonucleoproteins via magnetic peptide-imprinted chitosan nanoparticles. *Materials Today Bio*, *9*, 100091. https://doi.org/10.1016/J.MTBIO.2020.100091

McBain, S. C., Yiu, H. H. P., & Dobson, J. (2008). Magnetic nanoparticles for gene and drug delivery. *International Journal of Nanomedicine*, *3*(2), 169–180. https://doi.org/10.2147/ijn.s1608

Ozder, M., & Akbaba, H. (2021). Optimization and screening of solid lipid nanoparticle production for gene delivery by factorial design and response surface methodology. *Experimental Biomedical Research*, *4*(1), 23–37. https://doi.org/10.30714/j-ebr.2021165779

Schmidts, T., Dobler, D., Guldan, A. C., Paulus, N., & Runkel, F. (2010). Multiple W/O/W emulsions-Using the required HLB for emulsifier evaluation. *Colloids and Surfaces A: Physicochemical and Engineering Aspects*, *372*(1–3), 48–54. https://doi.org/10.1016/j.colsurfa.2010.09.025

Selmani, A., Kovačević, D., & Bohinc, K. (2022). Nanoparticles: From synthesis to applications and beyond. *Advances in Colloid and Interface Science*, *303*, 102640. https://doi.org/10.1016/J.CIS.2022.102640

Sharma, D., Arora, S., Singh, J., & Layek, B. (2021). A review of the tortuous path of nonviral gene delivery and recent progress. *International Journal of Biological Macromolecules*, *183*, 2055–2073. https://doi.org/10.1016/J.IJBIOMAC.2021.05.192

Song, H. P., Yang, J. Y., Lo, S. L., Wang, Y., Fan, W. M., Tang, X. S., Xue, J. M., & Wang, S. (2010). Gene transfer using self-assembled ternary complexes of cationic magnetic nanoparticles, plasmid DNA and cell-penetrating tat peptide. *Biomaterials*, *31*(4), 769–778. https://doi.org/10.1016/J.BIOMATERIALS.2009.09.085

Sun, C., Lee, J. S. H., & Zhang, M. (2008). Magnetic nanoparticles in MR imaging and drug delivery. *Advanced Drug Delivery Reviews*, *60*(11), 1252–1265. https://doi.org/10.1016/j.addr.2008.03.018

Tombácz, E., Turcu, R., Socoliuc, V., & Vékás, L. (2015). Magnetic iron oxide nanoparticles: Recent trends in design and synthesis of magnetoresponsive nanosystems. *Biochemical and Biophysical Research Communications*, *468*(3), 442–453. https://doi.org/10.1016/j.bbrc.2015.08.030

Zhi, J., Wang, Y., Lu, Y., Ma, J., & Luo, G. (2006). In situ preparation of magnetic chitosan/Fe3O4 composite nanoparticles in tiny pools of water-in-oil microemulsion. *Reactive and Functional Polymers*, *66*(12), 1552–1558. https://doi.org/10.1016/j.reactfunctpolym.2006.05.006